



ALMA MATER STUDIORUM  
UNIVERSITÀ DI BOLOGNA

ARCHIVIO ISTITUZIONALE  
DELLA RICERCA

## Alma Mater Studiorum Università di Bologna Archivio istituzionale della ricerca

Indomethacin co-crystals and their parent mixtures: does the intestinal barrier recognize them differently?

This is the final peer-reviewed author's accepted manuscript (postprint) of the following publication:

*Published Version:*

Ferretti, V., Dalpiaz, A., Bertolasi, V., Ferraro, L., Beggiato, S., Spizzo, F., et al. (2015). Indomethacin co-crystals and their parent mixtures: does the intestinal barrier recognize them differently?. *MOLECULAR PHARMACOLOGY*, 12(5), 1501-1511 [10.1021/mp500826y].

*Availability:*

This version is available at: <https://hdl.handle.net/11585/553229> since: 2016-07-15

*Published:*

DOI: <http://doi.org/10.1021/mp500826y>

*Terms of use:*

Some rights reserved. The terms and conditions for the reuse of this version of the manuscript are specified in the publishing policy. For all terms of use and more information see the publisher's website.

This item was downloaded from IRIS Università di Bologna (<https://cris.unibo.it/>).  
When citing, please refer to the published version.

(Article begins on next page)

This is the final peer-reviewed accepted manuscript of

Ferretti, V; Dalpiaz, A; Bertolasi, V; Ferraro, L; Beggiato, S; Spizzo, F; SPISNI, ENZO; Pavan, B.: Indomethacin co-crystals and their parent mixtures: does the intestinal barrier recognize them differently? MOLECULAR PHARMACOLOGY 12. ISSN 0026-895X

DOI: 10.1021/mp500826y

The final published version is available online at: <http://dx.doi.org/10.1021/mp500826y>

**Rights / License:** The terms and conditions for the reuse of this version of the manuscript are specified in the publishing policy. For all terms of use and more information see the publisher's website.

*This item was downloaded from IRIS Università di Bologna (<https://cris.unibo.it/>)*

***When citing, please refer to the published version.***

**Indomethacin Co-Crystals and their Parent Mixtures:  
does the Intestinal Barrier Recognize them Differently?**

Valeria Ferretti<sup>†</sup>, Alessandro Dalpiaz<sup>†,\*</sup>, Valerio Bertolasi<sup>†</sup>, Luca Ferraro<sup>‡</sup>, Sarah Beggiato<sup>‡</sup>, Federico Spizzo<sup>#</sup>, Enzo Spisni<sup>§</sup> and Barbara Pavan<sup>‡</sup>

<sup>†</sup>Department of Chemical and Pharmaceutical Sciences, University of Ferrara, Ferrara, Italy

<sup>‡</sup>Department of Life Sciences and Biotechnology, University of Ferrara, Ferrara, Italy

<sup>#</sup>Department of Physics and Earth Sciences, University of Ferrara, Ferrara, Italy

<sup>§</sup>Department of Biological, Geological and Environmental Sciences, University of Bologna, Bologna, Italy

**ABSTRACT:** Co-crystals are crystalline complexes of two or more molecules bound together in crystal lattices through non-covalent interactions. The solubility and dissolution properties of co-crystals can allow to increase the bioavailability of poorly water soluble active pharmaceutical ingredients (APIs). It is currently believed that the co-crystallization strategy should not induce changes on the pharmacological profile of the APIs, even if it is not yet clear whether a co-crystal would be defined as a physical mixture or as a new chemical entity. In order to clarify these aspects, we chose indomethacin as guest poorly aqueous soluble molecule and compared its properties with those of its co-crystals obtained with 2-hydroxy-4-methyl-pyridine (co-crystal *1*), 2-methoxy-5-nitroaniline (co-crystal *2*) and saccharine (co-crystal *3*). In particular, we performed a systematic comparison among indomethacin, its co-crystals and their parent physical mixtures by evaluating via HPLC analysis the API dissolution profile, its ability to permeate across intestinal cell monolayers (NCM460) and its oral bioavailability in rat. The indomethacin dissolution profile was not altered by the presence of co-crystallizing agents as physical mixtures, whereas significant changes were observed by the dissolution of the co-crystals. Furthermore, there was a qualitative concordance between the API dissolution patterns and the relative oral bioavailabilities in rats. Co-crystal *1* induced a drastic decrease of the transepithelial electrical resistance (TEER) value of NCM460 cell monolayers, whereas its parent mixture did not evidence any effect. The saccharin-indomethacin mixture induced a drastic decrease of the TEER value of monolayers, whereas its parent co-crystal *3* did not induce any effects on their integrity, being anyway able to increase the permeation of indomethacin. Taken together, these results demonstrate for the first time different effects induced by co-crystals and their parent physical mixtures on a biologic system, findings that could raise serious concerns about the use of co-crystal strategy to improve API bioavailability without performing appropriate investigations.

**KEYWORDS:** *co-crystals, indomethacin, saccharin, drug permeation, NCM 460 cells, bioavailability*

## INTRODUCTION

The therapeutic efficacy of a pharmaceutical formulation depends on its bioavailability, i.e. the absorption extent and rate of the active pharmaceutical ingredient (API) into the bloodstream following its administration. The bioavailability of a solid pharmaceutical formulation may depend in turn on the dissolution profile of its components, in particular of the API. In the case of highly lipophilic API, and therefore of a compound poorly soluble in water but capable of effectively permeate through biological membranes (Biopharmaceutical Classification System - BCS - class II), the dissolution process is the limiting factor of its absorption; in this case the bioavailability is highly dependent on both dissolution rate and maximum amount dissolved of the APIs themselves.<sup>1</sup>

The solid state form of an API is determinant in influencing its solubility and dissolution rate. In general, the amorphous phases are easier to solubilize than crystalline solids and, among them, the metastable polymorphs can offer solubility or dissolution advantages with respect to stable ones.<sup>2,3</sup>

The crystal engineering of pharmaceutical solids may be very useful to optimize the API stability and bioavailability, and the co-crystals seem to be promising in this context.<sup>4</sup> A co-crystal can be considered as a crystalline complex of two or more molecules bound together in the crystal lattice through non-covalent interactions, often including hydrogen bonding. Pharmaceutical co-crystals are obtained by an API and a co-crystal former.<sup>5</sup> It is known that the solubility and dissolution properties of co-crystals can be similar to those of amorphous compounds, *i.e.* higher than the parent crystalline pure phases. As a consequence, pharmaceutical co-crystals give the opportunities to increase bioavailability of APIs showing, at the same time, the stability of their stable crystalline forms.<sup>6,7</sup>

Currently, several APIs are known to improve their solubility profile and bioavailability when co-crystallized.<sup>7-9</sup> These APIs include the anticonvulsant carbamazepine,<sup>10</sup> nonsteroidal anti-

inflammatory drugs such as indomethacin and meloxicam,<sup>11,12</sup> the flavonoid quercetin,<sup>13</sup> or other molecules employed as model drugs.<sup>14-17</sup>

It is currently believed that the co-crystallization strategy should not induce changes on the pharmacological profile of the APIs. Indeed, co-crystal design requires changes on crystal structures that essentially alter hydrogen bonding motifs rather than covalent bonds of the API, thus retaining its safety and therapeutic properties.<sup>11,18</sup> On the other hand, the regulatory status regarding the use of co-crystals in pharmaceutical products appears still unsettled. In particular, it is not yet clear whether a co-crystal would be defined as a physical mixture (enabling its classification within current compendial guidelines) or as a new chemical entity requiring full safety and toxicology testing.<sup>7,8</sup> In this context, FDA has taken the position that a co-crystal may be treated as a drug product intermediate.<sup>8</sup>

In this study we evaluated the properties of (i) indomethacin, chosen as guest molecule poorly soluble in aqueous environment,<sup>11</sup> (ii) its two new co-crystals with 2-hydroxy-4-methyl-pyridine in its keto form (co-crystal **1**), 2-methoxy-5-nitroaniline (co-crystal **2**) and (iii) a previously described indomethacin-saccharine co-crystal<sup>11,19</sup> (co-crystal **3**). The schematic representation of indomethacin and the co-formers are reported in Figure 1. In particular, the dissolution, the permeation across NCM460 cell monolayers employed as an *in vitro* model of human intestinal epithelial barrier, and the bioavailability after oral administration to rats of indomethacin, its co-crystals and their parent mixtures (**1**, **2** and **3**, respectively) have been investigated. Overall, the results indicate, for the first time, that strongly different effects on the integrity of intestinal cell monolayers can derive by the dissolution of co-crystals or their parent mixtures.

## MATERIALS AND METHODS

**Materials and Reagents.**  $\gamma$ -indomethacin, 2-hydroxy-4-methyl-pyridine, 2-methoxy-5-nitro-aniline, saccharine, methanol, acetonitrile, ethyl acetate, isoamyl acetate and water were high performance liquid chromatography (HPLC) grade from Sigma Aldrich (Milan, Italy). All other reagents and solvents were of analytical grade (Sigma-Aldrich). NCM-460 cells were kindly provided by Dr. Antonio Strillacci, University of Bologna, Italy. The male Sprague-Dawley rats were provided by Charles-River (Milan, Italy).

**Synthesis of Adducts.** Two new co-crystals containing the indomethacin API have been synthesized and characterized by X-ray crystallography: **Co-crystal 1**:  $\gamma$ -indomethacin and 2-hydroxy-4-methyl-pyridine 1:1; **Co-crystal 2**:  $\gamma$ -indomethacin and 2-methoxy-5-nitro-aniline 1:1. Two other co-crystals have been synthesized and characterized but not used in the present work because of their poor reproducibility: **Co-crystal a**:  $\gamma$ -indomethacin and 4-nitropyridine-N-oxide monohydrate 1:1:1; **Co-crystal b**:  $\gamma$ -indomethacin and pyridine-N-oxide 1:1. Details of the X-ray crystallographic analysis for all the four crystals are reported in Supplementary Table 1. An equimolar quantity of indomethacin and co-crystal partner was dissolved in the minimum quantity of isoamyl acetate and left for slow evaporation at room temperature. Crystals were observed after a few days. **Co-crystal 3**, containing saccharine as the coformer, has been obtained by solvent slow evaporation of an equimolar saccharine/ $\gamma$ -indomethacin solution prepared according to ref. 19. The phase and composition of the co-crystals **1**, **2** and **3** have been checked by X-ray powder crystallography, comparing the experimental spectra with those calculated from the single-crystal crystallography structures (supplementary Figures. S1-S3)

**Experimental – X-Ray.** The crystallographic data for the four co-crystals **1**, **2**, **a**, **b** were collected on a Nonius Kappa CCD diffractometer at room temperature using graphite-monochromated

MoK $\alpha$  radiation ( $\lambda = 0.71073 \text{ \AA}$ ). Data sets were integrated with the Denzo-SMN package<sup>20</sup> and corrected for Lorentz-polarization effects. The structures were solved by direct methods with the SIR97 suite of programs<sup>21</sup> and refinement was performed on  $F^2$  by full-matrix least-squares methods with all non-hydrogen atoms anisotropic. The N/O-H atoms were found in the difference Fourier map and refined isotropically; all other hydrogen atoms were included on calculated positions, riding on their carrier atoms. All calculations were performed using SHELXL-97<sup>22</sup> implemented in the WINGX system of programs.<sup>23</sup> The ORTEPIII<sup>24</sup> diagrams of co-crystals **1** and **2** are shown in Figure 2. Powder diffraction spectra for co-crystals **1**, **2** and **3** were recorded, at room temperature, on a Bruker D-8 Advance diffractometer with graphite monochromatized Cu K $\alpha$  radiation ( $\lambda = 1.5406 \text{ \AA}$ ). The data were recorded at  $2\theta$  steps of  $0.02^\circ$  with 1 s/step. Crystallographic data for the structural analysis of the four new compounds have been deposited at the Cambridge Crystallographic Data Center, 12 Union Road, Cambridge, CB2 1EZ, UK, and are available free of charge from the Director on request quoting the deposition number CCDC 1005832-1005835 for **1**, **2**, **a** and **b**, respectively.

**Differential Scanning Calorimetry (DSC).** Thermal analyses on the samples were performed on a Perkin Elmer Differential Scanning Calorimeter DSC7; temperature and heat calibration were done using indium and zinc standards. The samples (4 - 6 mg) were put in non-hermetic aluminum pans and scanned at a heating rate of  $10 \text{ }^\circ\text{C}/\text{min}$  in the  $30 - 300 \text{ }^\circ\text{C}$  range under a continuous purged dry nitrogen atmosphere. The data were collected in triplicate for each sample.

**HPLC Analysis.** The quantification of the indomethacin was performed by HPLC. The chromatographic apparatus consisted of a modular system (model LC-10 AD VD pump and model SPD- 10A VP variable wavelength UV-vis detector; Shimadzu, Kyoto, Japan) and an injection valve with  $20 \text{ }\mu\text{L}$  sample loop (model 7725; Rheodyne, IDEX, Torrance, CA, USA). Separation was performed at room temperature on a reverse phase column Hypersil BDS C-18, 5U, equipped with a guard column packed with the same Hypersil material (Alltech Italia Srl BV, Milan, Italy). Data

acquisition and processing were accomplished with a personal computer using CLASS-VP Software, version 7.2.1 (Shimadzu Italia, Milan, Italy). The detector was set at 319 nm. The mobile phase consisted of a mixture of methanol and 0.2 phosphoric acid (75:25 v/v). The flow rate was 1 mL/min. The compound 9-phenyl- carbazole was employed as internal standard in extraction procedures of indomethacin from rat blood (see below). The retention times for indomethacin and 9-phenyl-carbazole were 4.0 and 13.5 minutes, respectively.

The chromatographic precision for each compound was evaluated by repeated analysis ( $n = 6$ ) of the same samples (100  $\mu\text{M}$ ). For indomethacin and 9-phenyl-carbazole (employed as internal standard in the extraction procedures) dissolved in aqueous phase the values were obtained for 100  $\mu\text{M}$  (0.036 mg/ml) solutions and were represented by the relative standard deviation (RSD) values ranging between 0.63% and 0.74%, respectively.

The calibration curves of indomethacin dissolved in phosphate buffer 200 mM and in PBS 10 mM were linear over the ranges of 50  $\mu\text{M}$  (0.018 mg/ml) - 1500  $\mu\text{M}$  (0.54 mg/ml) and 2  $\mu\text{M}$  (0.00072 mg/ml) – 500  $\mu\text{M}$  (0.18 mg/ml), respectively ( $n = 8$ ,  $r > 0.997$ ,  $P < 0,0001$ ). The limit of quantification for indomethacin was 625 nM (224 ng/ml, 2.24 ng injected) with a signal-to-noise ratio of 10, whereas the limit of detection was 188 nM (67 ng/ml, 0.67 ng injected) with a signal-to-noise ratio of 3.

A preliminary analysis performed with 100  $\mu\text{M}$  solutions showed that hydroxy-4-methyl-pyridine, 2-methoxy-5-nitro-aniline and saccharin did not interfere with the indomethacin and 9-phenylcarbazone retention times.

**Dissolution Studies.** For the dissolution studies, the samples were micronized and sieved using stainless steel standard-mesh sieves (mesh size 106  $\mu\text{m}$ ). In each experiment, the solid powders were added to 12 ml of phosphate buffer 200 mM and incubated at 37°C under gentle shaking (100 rpm) in a water bath. The amounts of sieved samples added to the buffer solution were 57.6 mg of

indomethacin; 75.2 mg of co-crystal **1**; 84.7 of co-crystal **2**; 86.9 of co-crystal **3**; 57.6 mg of indomethacin mixed with 17.6 of 2-hydroxy-4-methyl-pyridine, or 27.1 mg of 2-methoxy-5-nitro-aniline or 29.3 mg of saccharin for mixtures **1**, **2** or **3**, respectively. Aliquots (200  $\mu$ L) were withdrawn from the resulting slurry at fixed time intervals and filtered through regenerated cellulose filters (0.45  $\mu$ m). The resulting filtered samples were diluted 1:10 in water, then 10  $\mu$ l was injected into the HPLC system in order to quantify the indomethacin concentrations.

Dissolution experiments were conducted also in PBS 10 mM at 37°C with the same procedure above described, with the only difference that the filtered samples obtained from the slurry of mixture **3** were not diluted 1:10, but directly injected into the HPLC system. All the values obtained were the mean of three independent experiments.

**Cell Culture.** The NCM460 cell line was grown in DMEM + Glutamax supplemented with 10 % fetal bovine serum (FBS), 100 U/mL penicillin and 100 g/mL streptomycin at 37 °C in a humidified atmosphere of 95%, with 5% of CO<sub>2</sub>. For maximum viability, NCM460 cells were subcultured in fresh and spent growth medium in 1:1 ratio. All cell culture reagents were provided by Invitrogen (Life Technologies, Milan, Italy).

**Differentiation of NCM460 Cells to Polarized Monolayers.** Differentiation to NCM460 cell monolayers was performed modifying the method reported by Dalpiaz and co-workers.<sup>25</sup> Briefly, after two passages, confluent NCM460 cells were seeded at a density of 10<sup>5</sup> cells/mL in 1:1 ratio fresh and spent culture medium in 12-well Millicell inserts (Millipore, Milan, Italy) consisting of 1.0  $\mu$ m pore size polyethylene terephthalate (PET) filter membranes, whose surface was 1.12 cm<sup>2</sup>. Filters were presoaked for 24 h with fresh culture medium, and then the upper compartment (apical, A) received 400  $\mu$ L of the diluted cells, whereas the lower (basolateral, B) received 2 mL of the medium in the absence of cells. Half volume of the culture medium was replaced every two days with fresh medium to each of the apical and basolateral compartments. The integrity of the cell monolayers was monitored by

measuring the transepithelial electrical resistance (TEER) by means of a voltmeter (Millicell-ERS; Millipore, Milan, Italy). The measured resistance value was multiplied by the area of the filter to obtain an absolute value of TEER, expressed as  $\Omega \cdot \text{cm}^2$ . The background resistance of blank inserts not plated with cells was around  $35 \Omega \cdot \text{cm}^2$  and was deducted from each value. The homogeneity and integrity of the cell monolayer were also monitored by phase contrast microscopy. Based on these parameters, cell monolayers reached confluence and epithelial polarization after 6 days and monolayers with TEER stable value around  $180 \Omega \cdot \text{cm}^2$  were used for permeation studies. At this time, the medium was replaced with low serum fresh medium (1 % FBS) in both the apical and basal compartments.

**Permeation Studies Across Cell Monolayers.** For permeation studies, inserts were washed twice with pre-warmed PBS buffer in the apical compartment (A, 400  $\mu\text{L}$ ) and basolateral (B, 2 ml), then PBS buffer containing 5 mM glucose at  $37^\circ \text{C}$  was added to the apical compartment. The sieved powders (mesh size 106  $\mu\text{m}$ ) were added to the apical compartments in the following amounts: 1.92 mg of indomethacin; 2.5 mg of co-crystal **1**; 2.8 mg of co-crystal **2**; 2.9 of mg co-crystal **3**; 1.92 mg of indomethacin mixed to 0.59 mg of 2-hydroxy- 4 -methyl- pyridine, or 0.90 mg of 2 -methoxy-5-nitro-aniline, or 0.98 mg of saccharin for mixtures **1**, **2** or **3**, respectively. During permeation experiments, Millicell inserts loaded with the powders were continuously swirled on an orbital shaker (100 rpm; model 711/CT, ASAL, Cernusco, Milan, Italy) at  $37^\circ \text{C}$ . At programmed time points the inserts were removed and transferred into the subsequent wells containing fresh PBS, then basolateral PBS was harvested, filtered through regenerated cellulose filters (0.45  $\mu\text{m}$ ) and injected (10  $\mu\text{L}$ ) into the HPLC system for the determination of the concentration of indomethacin.

At the end of incubation the apical slurries were withdrawn, filtered and injected into HPLC system (10  $\mu\text{l}$ ) after 1:10 dilution, with the exception of the apical sample of the mixture **3** that was

directly injected after filtration, without dilution. After the withdrawn of apical samples, 400 µl of PBS were inserted in the apical compartments and TEER measurements were performed.

Permeation experiments were also conducted using cell-free inserts in the same conditions described above. All the values obtained were the mean of three independent experiments.

Apparent permeability coefficients ( $P_{app}$ ) of indomethacin were calculated according to the following equation:<sup>26-28</sup>

$$P_{app} = \frac{\frac{dc}{dt} V_r}{S_A C} \quad (1)$$

where  $P_{app}$  is the apparent permeability coefficient in cm/min;  $dc/dt$  is the flux of drug across the filters, calculated as the linearly regressed slope through linear data;  $V_r$  is the volume in the receiving compartment (basolateral = 2 mL);  $S_A$  is the diffusion area (1.13 cm<sup>2</sup>); and  $C$  is the compound concentration in the donor chamber (apical) detected at 60 min and chosen as approximate apical concentration.

**Statistical Analysis about Permeation Studies.** Statistical comparisons between apparent permeability coefficients or between apical concentrations of indomethacin were performed by one way ANOVA followed by Dunnett's post-test; statistical comparisons between transepithelial electrical resistance before and after incubation with the sieved samples was performed by one way ANOVA followed by Bonferroni post-test.  $P < 0.001$  was considered statistically significant. All the calculations were performed by using the computer program Graph Pad Prism (GraphPad Software Incorporated, La Jolla, CA, USA) that was employed also for the linear regression of the cumulative amounts of the compounds in the basolateral compartments of the Millicell systems. The quality of fit was determined by evaluating the correlation coefficients ( $r$ ) and  $P$  values.

***In Vivo* Administration of Indomethacin: Intravenous Infusion.** Male Sprague Dawley rats (200–250 g) kept fasting since 24 hours received a femoral intravenous infusion of 0.90 mg/mL

indomethacin dissolved in a medium constituted by 20% (v/v) DMSO and 80% (v/v) physiologic solution, with a rate of 0.2 mL/min for 5 min. Four rats were employed for femoral intravenous infusions. At the end of infusion and at fixed time points within 24 hours blood samples (300  $\mu$ L) were collected and inserted in heparinized test tubes that were centrifuged at 4°C for 15 min at 1,500 x g; 100  $\mu$ L of plasma were then withdrawn and immediately quenched in 300  $\mu$ L of ethanol (4 °C); 100  $\mu$ L of internal standard (100  $\mu$ M 9-phenyl-carbazole dissolved in ethanol) was then added. After centrifugation at 13,000 x g for 10 min, 400  $\mu$ L aliquots were reduced to dryness under a nitrogen stream and stored at -20° C until analysis. The samples were dissolved in 150  $\mu$ L of mobile phase (methanol and 0.2 phosphoric acid 75:25 v/v), and, after centrifugation, 10  $\mu$ L was injected into the HPLC system for indomethacin assay. All the values obtained were the mean of four independent experiments.

The efficacy of indomethacin extraction from blood samples was determined by recovery experiments, comparing the peak areas extracted from 10  $\mu$ M (3.58  $\mu$ g/ml) blood test samples at 4 °C with those obtained by injection of an equivalent concentration of the drug dissolved in their mobile phase. The average recovery  $\pm$  SD of indomethacin from rat blood resulted 87,4  $\pm$  3.9%. The concentrations of this compound were therefore referred to as peak area ratio with respect to the internal standard 9-phenyl-carbazole. The precision of the method based on peak area ratio, calculated for 10  $\mu$ M (3.6  $\mu$ g/ml) solutions, was represented by RSD values of 0.93% . The calibration of indomethacin was performed by employing eight different concentrations in whole blood at 4 °C ranging from 2  $\mu$ M (0.72  $\mu$ g/ml) to 50  $\mu$ M (18.0  $\mu$ g/ml) and expressed as peak area ratios of the compounds to the internal standard versus concentration. The calibration curve resulted linear (n = 8, r = 0.990, P < 0.0001). The accuracy of extraction method was determined with respect to the calibration curve and was described by relative errors comprised between -2.63% and 0.24%.

The *in vivo* half-life of indomethacin in the blood was calculated by nonlinear regression (exponential decay) of concentration values in the time range within 24 hours after infusion and confirmed by linear regression of the log concentration values versus time. The area under the concentration-time curve (AUC) value was calculated by the trapezoidal method within 24 hours, the remaining area was determined as the ratio between the indomethacin concentration detected at 24 hour and the elimination constant ( $k_{el}$ ), that was obtained from the slope of the semilogarithmic (-slope · 2.3). All the calculations were performed by using the computer program Graph Pad Prism.

***In Vivo Administration: Oral Administration of Indomethacin, its Co-Crystals and Parent Mixtures.*** The sieved powders were mixed with palatable food in order to induce their oral assumption by male Sprague Dawley rats (200–250 g) kept fasting since 24 hours. The following doses were administered: 0.90 mg of indomethacin; 1.18 mg of co-crystal *1*; 1.32 mg of co-crystal *2*; 1.36 mg of co-crystal *3*; 0.90 mg of indomethacin mixed to 0.28 mg of 2-hydroxy-4-methyl-pyridine, or 0.42 mg of 2-methoxy-5-nitro-aniline, or 0.46 mg of saccharin for mixtures *1*, *2* or *3*, respectively. Four rats/group were employed for the oral administration experiments. At the end of administration and at fixed time points within 24 hours blood samples (300  $\mu$ L) were collected, then extracted and analyzed as above described. All the concentration values obtained for indomethacin were the mean of four independent experiments. The AUC values referred to each orally administered treatment were calculated as above described. The absolute bioavailability values of indomethacin, referred to the oral administered samples, were obtained as the ratio between their oral AUC values and AUC of the intravenous administration of the drug. All the calculations were performed by using the computer program Graph Pad Prism.

**Statistical Analysis about *in Vivo* Administration of Indomethacin.** Statistical comparisons between absolute bioavailability values were performed by one way ANOVA followed by Dunnet

post-test.  $P < 0.001$  was considered statistically significant. All the calculations were performed by using the computer program Graph Pad Prism.

## RESULTS

**Indomethacin Co-Crystals.** Indomethacin was co-crystallized with two model molecules, 2-hydroxy-4-methyl-pyridine in its keto form (co-crystal **1**), 2-methoxy-5-nitroaniline (co-crystal **2**). Their chemical structures along with that of the previously reported<sup>11,19</sup> indomethacin-saccharin co-crystal (co-crystal **3**) are reported in Figure 1. The X-ray three-dimensional structures for the three co-crystals are shown in Figure 2, which evidences that the covalent bonds of each single molecule are not altered in the co-crystallized structures and shows the main hydrogen bonding interactions between indomethacin and co-crystallizing agents (dashed lines). In **1**, the pyridine derivatives are linked in dimers by N1A – H $\cdots$ O1A hydrogen bonds (Table 3 of the supplementary material) and each dimer, in turn, is linked on both sides to two indomethacin molecules through O3 – H $\cdots$ O1A hydrogen bonds involving the indomethacin carboxylic group (Figure 2a). In **2**, the indomethacin molecules are coupled in dimeric units by O3 – H $\cdots$ O4 hydrogen bonds, as found in the crystal lattice of the pure  $\gamma$ -indomethacin crystal.<sup>29</sup> The dimers link the cofomer molecules through the O1 chetonic oxygen, forming N-H $\cdots$ O interactions of medium strength (Figure 2b). In **3**, the indomethacin and saccharin molecules form in the crystal carboxylic acid and imide centrosymmetric dimers, respectively, resembling the arrangements found in the pure crystals.<sup>29,30</sup> The different dimers interact *via* a number of weak C-H $\cdots$ O/Cl interactions; the most relevant of them is shown in Figure 2c (C $\cdots$ Cl distance: 3.54 Å). More details about the crystal structures and the packing arrangements can be found in the supplementary material.

**DSC Analysis.** The DSC traces and thermal data for  $\gamma$ -indomethacin and its co-crystals are presented in Figure 3. Indomethacin showed a single melting transition with  $T_{max} = 160.8$  °C and enthalpy ( $\Delta H_f$ ) = 38.42 kJ/mole (Figure 3 and Table 1). The DSC thermogram for co-crystals **1**, **2** and **3** showed marked endothermic transitions attributed to the melting transition at  $T_{max} = 141.7, 118.9, 184.6$  °C, respectively (Figure 3 and Table 1). The related  $\Delta H_f$  values were 66.16 kJ/mol for co-crystal **1**, 55.75 kJ/mol for co-crystal **2** and 77.46 kJ/mol for co-crystal **3**.

**Dissolution Studies: Co-Crystals Can Significantly Change the Dissolution Profiles of Indomethacin.** Figure 4A reports a comparison between the dissolution profiles in 200 mM phosphate buffer at 37°C of  $\gamma$ -indomethacin, as free drug, co-crystallized or mixed in the parent mixtures. The saturation concentration of free  $\gamma$ -indomethacin, reached after about two hours of its incubation into the buffer, was about 1.8 mg/ml. The dissolution profile of  $\gamma$ -indomethacin was not altered by the presence of the co-crystallizing agents when mixed with the drug. Differently, the co-crystallized powders induced significant changes of indomethacin dissolution profiles. In particular, the co-crystal **1** and the co-crystal **2** induced an increase up to three times and a 50% decrease of  $\gamma$ -indomethacin saturation concentration, respectively, without affecting the dissolution rate. Finally, the co-crystal **3** induced not only a significant enhancement of the saturation concentration of  $\gamma$ -indomethacin (up to four times) but, differently from the other co-crystals, also an increase of the drug dissolution rate, being 30 min the time necessary to reach the saturation conditions.

The indomethacin solubility and dissolution profiles represented in Figure 4A drastically changed when the powders were incubated in PBS 10 mM, the medium employed for the drug permeation studies across NCM460 cell monolayers (see below). In particular, under these experimental conditions, the saturation concentration of free  $\gamma$ -indomethacin was reduced of about 50% when compared to that measured when it was dissolved in 200 mM phosphate buffer (Figure 4B); the

mixtures **1** and **2** showed dissolution profiles similar to that of free  $\gamma$ -indomethacin, whereas the mixture **3** induced a drastic decrease of the saturation concentration of the drug, showing a mean  $\pm$  S.D value of  $0.0012 \pm 0.0004$  mg/ml (about 0.2% of the saturation concentration of the free drug). The co-crystal **1** was instead associated to an increase of indomethacin saturation concentration. Differently from the results obtained under 200 mM phosphate buffer conditions (see above), the co-crystal **2** led to an indomethacin dissolution profile similar to those displayed by the free drug. Finally, the co-crystal **3** induced a very fast dissolution of indomethacin that was, however, followed by a sudden precipitation of the drug; this event was completed within 60 minutes, showing indomethacin concentration values about 0.003 mg/ml.

#### **Permeation Studies: Co-Crystals Can Induce Different Effects on Cell Monolayers with Respect to their Parent Mixtures**

The PBS was used as incubation medium for the permeation studies of indomethacin across an *in vitro* model of human intestinal wall, i.e. NCM460 cell monolayers.<sup>31</sup> In order to simulate an oral administration, the powders of  $\gamma$ -indomethacin, its co-crystals or the parent mixtures were introduced in the apical compartment of the “millicell” systems with the same ratio between solid powders and incubation medium adopted for dissolution studies. The indomethacin permeation profiles, expressed by the cumulative concentrations in the receiving basolateral compartments are reported in Figure 5. The linear profiles indicate constant permeation conditions during the analysis time period (60 min) for all samples. The straight line related to mixture **3** ( $r = 0.970$ ,  $P = 0.001$ ) was characterized by indomethacin concentration values strongly lower than those of the straight lines of the other powders ( $r \geq 0.998$ ,  $P < 0.0001$ ). The apparent permeability coefficients ( $P_{app}$ ) of indomethacin (Table 2) have been calculated on the basis of the resulting slopes of the linear fits and the indomethacin concentrations detected in the apical compartments after one hour of incubation of the powders (Table 2), chosen as approximate apical concentrations. These latter values appeared essentially in line with

those obtained from dissolution studies of indomethacin powders in 10 mM PBS (Figure 4B). Indeed, the drug concentrations obtained from the powders constituted by  $\gamma$ -indomethacin, mixtures **1** and **2** and co-crystal **2** were not statistically dissimilar among them (about 1000  $\mu$ M,  $P > 0.05$ ). On the other hand, mixture **3** induced a drastic reduction of indomethacin concentration ( $P < 0.001$ ), showing values close to the drug limit of quantification. Furthermore, the co-crystal **1** induced an increase of indomethacin concentration of about three times with respect to the free drug powder ( $P < 0.001$ ), whereas the co-crystal **3** significantly reduced the  $\gamma$ -indomethacin concentration ( $P < 0.001$ ), even if in a less drastic manner than detected from dissolution experiments in 10 mM PBS in the absence of cells (Figure 4B). The slope of the permeation profile (Figure 5) and the apical concentration of indomethacin related to mixture **3** (Table 2) appeared too low to obtain a reliable  $P_{app}$  value of indomethacin dissolved from this sample.

A comparison of the  $P_{app}$  values of  $\gamma$ -indomethacin (Table 2) obtained in the presence ( $150 \cdot 10^{-5} \pm 6 \cdot 10^{-5}$  cm/min) and in the absence ( $429 \cdot 10^{-5} \pm 18 \cdot 10^{-5}$  cm/min) of NCM460 cell monolayers indicated a significant lower permeation of the drug in the presence of cells ( $P < 0.001$ ), confirming the validity of the monolayer as an *in vitro* model of a physiologic barrier. This behavior appeared in agreement with the transepithelial electrical resistance (TEER) values (about  $180 \Omega \cdot \text{cm}^2$ ) attributed to the monolayers before their incubation with the powders (Table 2). The apparent coefficient values across the monolayer of indomethacin dissolved from mixtures **1** and **2** and co-crystal **2** did not significantly differ from the  $P_{app}$  obtained for the free  $\gamma$ -indomethacin (Table 2,  $P > 0.05$ ). On the other hand, the co-crystal **1** induced a consistent increase of indomethacin permeation ( $P_{app} = 301 \cdot 10^{-5} \pm 11 \cdot 10^{-5}$  cm/min,  $P < 0.001$ ). This phenomenon was associated to the ability of this co-crystal to impair the tight junctions among the cells of the monolayer. This ability was evidenced by the drastic reduction of TEER values ( $P < 0.001$ ) measured after 60 min of incubation with this sample ( $21 \pm 1 \Omega \cdot \text{cm}^2$ ) in

comparison to the value obtained before incubation ( $185 \pm 11$ ). Moreover, by monitoring the monolayer after its incubation with co-crystal **1** by phase contrast microscopy evidenced a complete separation of the cells (*data not shown*). It is remarkable that mixture **1** incubation did not alter neither the monolayer integrity, as monitored by phase contrast microscopy (*data not shown*) nor the TEER value (before incubation =  $181 \pm 9 \Omega \cdot \text{cm}^2$ ; after incubation =  $158 \pm 7 \Omega \cdot \text{cm}^2$ ;  $P > 0.05$ ). The same profile has been also registered for the powder of free  $\gamma$ -indomethacin, the mixture **2** and the co-crystals **2** and **3**. It is interesting to observe that the mixture **3** induced a cell monolayer fragmentation, as monitored by phase contrast microscopy (*data not shown*) and indicated by the TEER value (before incubation =  $180 \pm 10 \Omega \cdot \text{cm}^2$ ; after incubation =  $36 \pm 2 \Omega \cdot \text{cm}^2$ ;  $P < 0.001$ ). The co-crystal **3** has been characterized by a  $P_{\text{app}}$  value of  $374 \cdot 10^{-5} \pm 16 \cdot 10^{-5} \text{ cm/min}$ , significantly higher with respect to that obtained with the powder of free  $\gamma$ -indomethacin ( $P < 0.001$ ). Interestingly, the permeation enhancement induced by co-crystal **3** was not related with the monolayer fragmentation (*data not shown*).

***In Vivo* Administration of Indomethacin: its Oral Bioavailability is Modulated by Co-crystallization.** After intravenous infusion of 0.90 mg indomethacin, the drug concentration in the rat bloodstream was  $13.2 \pm 1.4 \mu\text{g/ml}$ . This value decreased during time with an apparent first order kinetic (Figure 6A) confirmed by the linearity of the semilogarithmic plot reported in the inset of Figure 6A ( $n = 8$ ,  $r = 0.983$ ,  $P < 0.0001$ ), showing an half-life value of  $8.94 \pm 0.38$  hours.

The rat blood indomethacin concentrations within 24 hours after its intravenous infusion (IV) as free-drug or the oral administration of 0.90 mg indomethacin as sieved powders of free  $\gamma$ -drug, its co-crystals and the parent mixtures are reported in Figure 6B. In order to better compare among them the results, Figure 6C reports a section of Figure 6B, focused on the profiles obtained within eight hours after of the oral administration of the powders. It can be observed that the free  $\gamma$ -indomethacin powder

induced a concentration peak in the rat bloodstream of about 5 µg/ml two hours after the administration. A similar profile was obtained with mixtures **1** and **2**, whereas mixture **3** was characterized by a profile showing a peak concentration of about 3.5 µg/ml two hours after its administration.

The co-crystal **1** induced a concentration peak in the rat bloodstream of about 5 µg/ml 30 minutes after the administration, the same time required for co-crystal **3** to induce a concentration peak of about 3 µg/ml. The co-crystal **2** profile was instead characterized by a peak lower than 2 µg/ml obtained between 1 and 2 hours after the administration. In general, the profiles of the co-crystals appeared characterized by a decrease of indomethacin blood concentration within 4 hours after their administration with a rate lower than those observed following free  $\gamma$ -indomethacin and the parent mixtures administrations.

The AUC values of the profiles reported in Figure 6B were employed for the calculation of absolute bioavailabilities (F) of the solid formulations, reported in Table 2. In particular the free  $\gamma$ -indomethacin powder was characterized by an F value of  $23.5 \pm 0.8\%$ , not statistically dissimilar ( $P > 0.05$ ) from those of mixtures **1**, **2** and **3**. The co-crystals **1** and **3** were characterized by a significant higher ( $P < 0.001$ ) F values than free  $\gamma$ -indomethacin ( $37.7 \pm 1.5\%$  and  $33.58 \pm 0.59\%$ , respectively), while, co-crystal **2** induced a relative small, but significant ( $P < 0.001$ ) decrease of bioavailability with respect to the powder of the free drug (F value =  $20.1 \pm 0.9\%$ ).

## **DISCUSSION**

Co-crystallization, by enhancing BCS class II API solubility, has been proposed as a new strategy to increase drug bioavailability.<sup>9-17</sup> However, experimental evidence about the effects of the

co-crystals on the permeation of APIs across intestinal barriers and on intestinal epithelial barrier integrity is not reported in literature. These studies should be relevant as the disruption of intestinal epithelial tight junctions has two undesirable consequences: unwanted substances such as endotoxins are allowed into the body, and depolarization of cells may be promoted.<sup>32,33</sup> Moreover, the regulatory status regarding the use of co-crystals in pharmaceutical products appears still unsettled, being necessary to clarify whether the co-crystal would be defined as a physical mixture or as a new chemical entity requiring full safety and toxicology testing.<sup>7,8</sup> In the attempt to contribute to clarify these aspects, we have chosen indomethacin as a model BCS class II API and compared its properties with those of three of its co-crystals along with their parent physical mixtures. To our knowledge, this type of study is absolutely novel, being not only focused to a systematic comparison among the behavior of powders constituted by the pure API, its co-crystals and their parent mixtures, but also involving the analysis of the API permeation across an *in vitro* intestinal barrier model.

The dissolution studies were firstly performed in a 200 mM phosphate buffer, pH 7.4. The relative high ionic strength of this buffer was necessary to maintain the stability of pH value during the dissolution processes.<sup>19</sup> As already described, we have observed that the dissolution profile of indomethacin was not altered by the presence of the co-crystallizing agents in the form of physical mixtures with the API, whereas significant changes were observed by the dissolution of the co-crystals. This behavior is consistent with the different crystal packing forces due to the different intermolecular interaction patterns of the considered crystals as described in the Results section. These differences are reflected by the different thermal behavior of the indomethacin and its co-crystals. In particular, the enthalpy data for  $\gamma$ -indomethacin and co-crystal **3** differ by about 39 kJ/mol, as previously reported;<sup>19</sup> in this case the higher lattice energy of **3** is related to a solubility higher than the pure indomethacin, similarly as it happens with co-crystal **1**. It is known<sup>34</sup> that the ideal solubility depends on the melting temperature and enthalpy of the solute; such behavior, however, only applies to specific cases, such as

polymorphs. On the contrary, melting points and related enthalpies values ‘*have often been shown to be poor parameters to judge aqueous solubility of co-crystals*’<sup>35</sup> indicating that the co-crystal solubility is dependent on more than a single factor.

A qualitative concordance between the API dissolution patterns in the 200 mM phosphate buffer and its absorption in the rat bloodstream after the oral administration of the powders, has been observed. In particular, dissolution (Figure 4A) and bioavailability (Figure 6C) profiles of pure  $\gamma$ -indomethacin were similar to those of its physical mixtures with the co-crystallizing molecules; on the other hand either indomethacin solubility or its bioavailability were significantly increased by co-crystals **1** and **3**, and weakly decreased by co-crystal **2**. It is worth noting that, to allow a direct comparison among the powder constituted by the free drug, its co-crystals and the parent mixtures we intentionally decided to do not follow the suitable formulation strategies suggested to improve the plasma levels of APIs orally administered as co-crystals.<sup>9</sup> This can explain the relatively weak, although significant, changes of bioavailability induced by the co-crystallization observed in the present study. However, the accordance between dissolution and bioavailability profiles above described is in line with literature data concerning pharmaceutical co-crystals.<sup>10-17</sup> Since this correlation does not provide any information on the effective role of the co-crystals in influencing the API absorption mechanisms across the intestinal barrier, we decided to perform permeation experiments across NCM460 cell monolayers. These studies are absolutely innovative for systems involving pharmaceutical co-crystals and their parent mixtures.

Various cell monolayer models that mimic the human intestinal epithelial barrier have been developed, providing ideal systems for the rapid *in vitro* assessment of the intestinal absorption of drug candidates. We have chosen the human normal colonic epithelial NCM460 cells being them an immortalized, non-transformed cell line, derived from primary cells of the normal human transverse colonic mucosa.<sup>29</sup> As these cells are not of tumor origin neither transfected ones, they retain more

closely the physiological characteristics of the normal human colon compared to the pathologically or experimentally transformed cell lines. In this context, it is worth noting that TEER developed by the NCM460 cells are within the range reported for intact sheets of human colonic mucosa.<sup>36,37</sup> Furthermore, the lipophilic nature of indomethacin enables the molecule to diffuse quickly and to get absorbed completely through the intestinal membrane after oral ingestion, resulting almost equally permeable in the colon and small intestine.<sup>38,39</sup>

The permeation studies were performed by glucose-enriched PBS as dissolution medium of the indomethacin powder, being the concentration of 200 mM phosphate buffer too high to allow the cell survival. Moreover, PBS represented the simplest medium where to dissolve indomethacin from its powders, in order to study the permeation properties across NCM460 cells in the absence of other interfering substances. It is indeed known that simulated intestinal buffers can induce TEER changes of the monolayers and have inhibitory activity towards efflux transporters expressed on the cell membranes.<sup>40</sup> As described above, the dissolution profiles in PBS of indomethacin showed some marked differences with respect to the patterns obtained in 200 mM phosphate buffer, attributable to the PBS relatively weak buffering power.

The suspensions obtained by the introduction of the solid powders containing indomethacin in the apical compartments of the “millicell” systems allowed us to simulate an oral administration. The  $\gamma$ -indomethacin crystals appeared able to maintain the integrity of the monolayer characterized by TEER values around  $180 \Omega \cdot \text{cm}^2$ . Moreover, a comparison of the permeability values obtained in the absence and in the presence of cell monolayer validated the ability of this preparation to behave as a physiologic barrier. We have instead observed that the physical mixture of indomethacin and saccharin induced a drastic decrease of the TEER value of the monolayer, whose cells appeared to lose completely their mutual contacts after one hour of incubation. Surprisingly, the incubation with the parent co-crystal **3** allowed to maintain the integrity of the monolayer as well as of its TEER value, and

induced an increase of indomethacin permeation across the NCM460 cells, with respect to  $\gamma$ -indomethacin crystals.

We have also observed that co-crystal **1** induced a drastic decrease of the TEER value of the monolayer, whose cells appeared completely separated after one hour of incubation. The permeation profile of indomethacin dissolved from co-crystal **1** showed indeed the highest values with respect to all other cases, probably due to both the loss of the barrier effect of the monolayer and the increased dissolution of the API. Surprisingly, the incubation with the parent physical mixture **1** did not induce any changes on the monolayer integrity, as evidenced by unaffected TEER value after one hour of incubation. Moreover, the permeation profile of indomethacin dissolved from this mixture was the same to that obtained with solid  $\gamma$ -indomethacin. No significant differences between  $\gamma$ -indomethacin and co-crystal **2** or mixture **2** were observed, as far as the integrity of the monolayer and API permeation profile is concerned.

## CONCLUSIONS

To the best of our knowledge this is the first study demonstrating different effects induced by co-crystals and their parent physical mixtures on a biologic system, findings that could raise serious concerns about the use of co-crystal strategy to improve API bioavailability without performing appropriate investigations. In this case co-crystal **1** was found to induce a drastic decrease of the TEER value NCM460 cell monolayers, whereas its parent mixture did not evidence any effect. On the other hand, the physical mixture of saccharin and indomethacin was able to induce a drastic decrease of the TEER value of NCM460 monolayers, whereas its parent co-crystal **3** did not evidence any effect on the integrity of the monolayers, being anyway able to increase the permeation of indomethacin across the monolayers. On the basis of the present experimental data we cannot explain the reason(s) of these

phenomena, but it is clearly evidenced that the biological effects of a co-crystal and its parent mixture can be drastically different, even if this is not to be taken as a general rule. Indeed, any difference was registered by our permeation measurements between co-crystal **2** and its parent physical mixture on NCM460 cell monolayer.

Our results seem to open new perspectives about the application of pharmaceutical products containing co-crystals. New and appropriate investigations appear therefore necessary in order to evaluate the potential new applications and the potential damaging effects of pharmaceutical co-crystals.

## AUTHOR INFORMATION

### Corresponding Author

\*Department of Chemical and Pharmaceutical Sciences, University of Ferrara, via Fossato di Mortara 19, I-44121, Ferrara, Italy. Phone: +39-0532-455274. Fax: +39-0532- 455953. E-mail: dla@unife.it.

## REFERENCES

- (1) Dressman, J.; Reppas, C. Drug Solubility: How to Measure it, how to Improve it. *Adv. Drug Del. Rev.* **2007**, 59, 531-532.
- (2) Morissette, S. L.; Soukasene, S.; Levinson, D.; Cima, M. J.; Almarsson O. Elucidation of Crystal form Diversity of the HIV Protease Inhibitor Ritonavir by High-Throughput crystallization. *Proc. Natl. Acad. Sci. U.S.A* **2003**, 100, 2180–2184.
- (3) Heinz, A.; Strachan, C. J.; Gordon, K. C.; Rades, T. Analysis of Solid-State Transformations of Pharmaceutical Compounds Using Vibrational Spectroscopy. *J. Pharm. Pharmacol.* **2009**, 61, 971–988.

- (4) Schultheiss, N.; Newman, A. Pharmaceutical Cocrystals and their Physicochemical Properties. *Cryst. Growth Des.* **2009**, *9*, 2950–2967.
- (5) Jones, W.; Motherwell, W. D. S.; Trask, A. V. Pharmaceutical Cocrystals: an Emerging Approach to Physical Property Enhancement. *MRS Bulletin* **2006**, *31*, 875-879.
- (6) Remenar, J. F.; Morissette, S. L.; Peterson, M. L.; Moulton, B.; MacPhee, J. M.; Guzman, H. R.; Almarsson, O. Crystal Engineering of Novel Cocrystals of a Triazole Drug with 1,4-Dicarboxylic Acids. *J. Am. Chem. Soc.* **2003**, *125*, 8456-8457.
- (7) Brittain, H. G. Cocrystal Systems of Pharmaceutical Interest: 2010. *Cryst. Growth Des.* **2012**, *12*, 1046–1054.
- (8) Brittain, H. G. Cocrystal Systems of Pharmaceutical Interest: 2011. *Cryst. Growth Des.* **2012**, *12*, 5823–5832.
- (9) Childs, S. L.; Kandi, P.; Lingireddy, S. R. Formulation of a Danazol Cocrystal with Controlled Supersaturation Plays an Essential role in Improving Bioavailability. *Mol. Pharm.* **2013**, *10*, 3112–3127.
- (10) Hickey, M. B.; Peterson, M. L.; Scopettuolo, L. A.; Morissette, S. L.; Vetter, A.; Guzman, H.; Remenar, J. F.; Zhang, Z.; Tawa, M. D.; Haley, S.; Zaworotko, M. J.; Almarsson, O. Performance Comparison of a Cocrystal of Carbamazepine with Marketed Product. *Eur. J. Pharm. Biopharm.* **2007**, *67*, 112–119.
- (11) Jung, M. S.; Kim, J. S.; Kim, M. S.; Alhalaweh, A.; Cho, W.; Hwang, S. J.; Velaga, S. P. Bioavailability of Indomethacin-Saccharin Cocrystals. *J. Pharm. Pharmacol.* **2010**, *62*, 1560–1568.
- (12) Weyna, D. R.; Cheney, M. L.; Shan, N.; Hanna, M.; Zaworotko, M. J.; Sava, V.; Song, S.; Sanchez-Ramos, J. R. Improving Solubility and Pharmacokinetics of Meloxicam via Multiple-Component Crystal Formation. *Mol. Pharm.* **2012**, *9*, 2094–2102.

- (13) Smith, A. J.; Kavuru, P.; Wojtas, L.; Zaworotko, M. J.; Shytle, R. D. Cocrystals of Quercetin with Improved Solubility and Oral Bioavailability. *Mol. Pharm.* **2011**, *8*, 1867–1876.
- (14) McNamara, D. P.; Childs, S. L.; Giordano, J.; Iarriccio, A.; Cassidy, J.; Shet, M. S.; Mannion, R.; O'Donnell, E.; Park, A. Use of a Glutaric Acid Cocrystal to Improve Oral Bioavailability of a low Solubility API. *Pharm. Res.* **2006**, *23*, 1888–1897.
- (15) Bak, A.; Gore, A.; Yanez, E.; Stanton, M.; Tufekcic, S.; Syed, R.; Akrami, A.; Rose, M.; Surapaneni, S.; Bostick, T.; King, A.; Neervannan, S.; Ostovic, D.; Koparkar, A. The Co-Crystal Approach to Improve the Exposure of a Water-Insoluble Compound: AMG 517 Sorbic Acid Co-Crystal Characterization and Pharmacokinetics. *J. Pharm. Sci.* **2008**, *97*, 3942–3956.
- (16) Stanton, M. K.; Kelly, R. C.; Colletti, A.; Langley, M.; Munson, E. J.; Peterson, M. L.; Roberts, J.; Wells, M. Improved Pharmacokinetics of AMG 517 through Co-Crystallization part 2: Analysis of 12 Carboxylic Acid Co-Crystals. *J. Pharm. Sci.* **2011**, *100*, 2734–2743.
- (17) Zheng, W.; Jain, A.; Papoutsakis, D.; Dannenfelser, R. M.; Panicucci, R.; Garad, S. Selection of Oral Bioavailability Enhancing Formulations during Drug Discovery. *Drug Dev. Ind. Pharm.* **2012**, *38*, 235–247.
- (18) Bethune, S. J.; Schultheiss N.; Henck, J. O. Improving the Poor Aqueous Solubility of Nutraceutical Compound Pterostilbene through Cocrystal Formation. *Cryst. Growth Des.* **2011**, *11*, 2817–2823.
- (19) Basavoju, S.; Bostrom, D.; Velaga, S. P. Indomethacin-Saccharin Cocrystals: Design, Synthesis and Preliminary Pharmaceutical Characterization. *Pharm. Res.* **2008**, *25*, 530-541.
- (20) Otwinowski, Z.; Minor, W. Processing of X-Ray Diffraction Data Collected in Oscillation Mode. In *Methods in Enzymology, 276, Macromolecular Crystallography, Part A*, Carter, C.W. Jr & Sweet, R.M. Eds., Academic Press: New York, 1997; pp 307-326

- (21) Altomare, A.; Burla, M. C.; Camalli, M.; Cascarano, G.; Giacovazzo, C.; Guagliardi, A.; Moliterni, A. G.; Polidori, G.; Spagna, R. SIR97: a New Tool for Crystal Structure Determination and Refinement. *J. Appl. Crystallogr.* **1999**, 32, 115–119.
- (22) Sheldrick, G. M. *SHELX97, Program for Crystal Structure Refinement*; University of Göttingen, Göttingen, Germany, 1997
- (23) Farrugia, L. J. WinGX Suite for Small-Molecule Single-Crystal Crystallography. *J. Appl. Crystallogr.* **1999**, 32, 837–838.
- (24) Burnett, M. N.; Johnson, C. K. *ORTEP III. Report ORNL-6895*; Oak Ridge National Laboratory, Oak Ridge, Tennessee, USA, 1996.
- (25) Dalpiaz, A.; Paganetto, G.; Pavan, B.; Fogagnolo, M.; Medici, A.; Beggiato, S.; Perrone, D. Zidovudine and Ursodeoxycholic Acid Conjugation: Design of a New Prodrug Potentially Able to Bypass the Active Efflux Transport Systems of the Central Nervous System. *Mol. Pharm.* **2012**, 9(4), 957-968.
- (26) Artursson, P.; Karlson, J. Correlation Between Oral Absorption in Humans and Apparent Drug Permeability Coefficients in Human Intestinal Epithelial (Caco-2) Cells. *Biochem. Biophys. Res. Commun.* **1991**, 175, 880–885.
- (27) Pal, D.; Udata, C.; Mitra, A. K. Transport of Cosalane, a Highly Lipophilic Novel Anti-HIV Agent, across Caco-2 Cell Monolayers. *J. Pharm. Sci.* **2000**, 89, 826–833.
- (28) Raje, S.; Cao, J.; Newman, A. H.; Gao, H.; Eddington, N. D. Evaluation of the Blood-Brain Barrier Transport, Population Pharmacokinetics, and Brain Distribution of Benzotropine Analogs and Cocaine Using in vitro and in vivo Techniques. *J. Pharmacol. Exp. Ther.* **2003**, 307, 801–808.
- (29) Kistenmacher, T.J.; Marsh, R. E. Crystal and Molecular Structure of an Antiinflammatory Agent, Indomethacin, 1-(p-chlorobenzoyl)-5-methoxy-2-methylindole-3-acetic acid. *J. Am. Chem. Soc.*, **1972**, 94, 1340-1345.

- (30) Wardell, J. L.; Low, J. N.; Glidewell, C. Saccharin, Redetermined at 120 K: a Three-dimensional Hydrogen-Bonded Framework. *Acta Crystallogr.*, **2005**, E61, o1944-o1946]
- (31) Moyer, M. P.; Manzano, L.; Merriman, R.; Stauffer, J.; Tanzer, L. R. NCM460, a Normal Human Colon Mucosal Epithelial Cell Line. *In Vitro Cell Dev. Biol. Anim.* **1996**, 32, 315–317.
- (32) Laurent-Puig, P.; Blons, H.; Cugnenc, P. H. Sequence of Molecular Genetic Events in Colorectal Tumorigenesis. *Eur. J. Cancer Prev.* **1999**, 8, Suppl 1, S39–S47.
- (33) Rao, R. K.; Seth, A.; Sheth P. Recent Advances in Alcoholic Liver Disease I. Role of Intestinal Permeability and Endotoxemia in Alcoholic Liver Disease. *Am. J Physiol. Gastrointest. Liver Physiol.* **2004**, 286, G881–G884.
- (34) Yalkowsky, S.H. *Solubility and Solubilization in Aqueous Media*, Am. Chem. Soc., Oxford University Press, New York, 1999
- (35) Roy, L.; Lipert, M.P.; Rodriguez-Hornedo, N. Co-crystal Solubility and Thermodynamic Stability. In *Pharmaceutical Salts and Co-crystals*, Wouters J., Quere L. Eds.; Royal Society of Chemistry, Cambridge, 2012; pp 247-279.
- (36) Sahi, J.; Nataraja, S. G.; Layden, T .J.; Goldstein, J. L.; Moyer, M. P.; Rao M. C. Cl<sup>-</sup> Transport in an Immortalized Human Epithelial Cell Line (NCM460) Derived from the Normal Transverse Colon. *Am. J. Physiol.* **1998**, 275 (4Pt1), C1048-1057.
- (37) Liu, Z. H.; Shen, T. Y.; Zhang P.; Ma, Y. L.; Moyer, M. P.; Qin, H. L. Protective Effects of Lactobacillus Plantarum against Epithelial Barrier Dysfunction of Human Colon Cell Line NCM460. *World J. Gastroenterol.* **2010**, 16, 5759-5765.
- (38) ElShaer, A.; Hanson, P.; Mohammed, A. R. A Novel Concentration Dependent Amino Acid Ion Pair Strategy to Mediate Drug Permeation using Indomethacin as a Model Insoluble Drug. *Eur. J. Pharm. Sci.* **2014**, 62, 124-131.

(39) Ehrhardt, C.; Kim K. J. *Drug Absorption Studies: In Situ, In Vitro and In Silico Models*.

Springer: New York, 2008.

(40) Ingels, F.; Defermec, S.; Destexhe, E.; Oth, M., Van den Mooter, G.; Augustijns, P.

Simulated Intestinal Fluid as Transport Medium in the Caco-2 Cell Culture Model. *Int. J. Pharm.* **2002**,

232, 183–192.

**Table 1.** Melting Points and Enthalpy Values for  $\gamma$ -indomethacin and its co-crystals. Data are reported as mean  $\pm$  S.D. of three independent experiments.

<b>Compound</b>	<b>Melting point (<math>^{\circ}</math>C)</b>	<b><math>\Delta H</math> (kJ/mol)</b>
$\gamma$ -indomethacin	160.8 $\pm$ 0.8	38.42 $\pm$ 0.11
Co-crystal 1	141.7 $\pm$ 0.3	66.16 $\pm$ 0.14
Co-crystal 2	118.9 $\pm$ 0.3	55.75 $\pm$ 1.05
Co-crystal 3	184.6 $\pm$ 0.4	77.46 $\pm$ 0.81

**Table 2.** Data related to indomethacin *in vitro* permeation studies and *in vivo* oral bioavailability.

Permeation studies were performed by using “millicell” filters alone (filter) or coated by NCM460 cell monolayers (cells). Indomethacin was introduced in the donor compartment as sieved powder of  $\gamma$ -indomethacin, or its co-crystals, or the parent mixtures. The apical concentrations detected at the end of incubation were employed for the calculation of the apparent permeation coefficients ( $P_{app}$ ). Permeation studies were performed after cell cultures reached the confluence using parallel sets of “millicell” well plates with similar TEER values (TEER 0 min). The TEER values were measured again at the end of incubation (TEER 60 min). All data related to permeation studies are reported as the mean  $\pm$  S.D. of three independent experiments. Bioavailability data were obtained after oral administration to rats of the powders and are reported as the mean  $\pm$  S.D. of four independent experiments.

<b>Powder</b>	<b>Permeation condition</b>	<b>Apical concentrations at 60 min (<math>\mu</math>M)</b>	<b><math>P_{app}</math> (<math>\cdot 10^{-5}</math> cm/min)</b>	<b>TEER (<math>\Omega \cdot \text{cm}^2</math>) 0 min</b>	<b>TEER (<math>\Omega \cdot \text{cm}^2</math>) 60 min</b>	<b>Absolute Bioavailability (%)</b>
$\gamma$ -Indomethacin	Cells	1010 $\pm$ 40	150 $\pm$ 6	181 $\pm$ 10	163 $\pm$ 8	23.5 $\pm$ 0.8
Mixture 1	Cells	989 $\pm$ 42	165 $\pm$ 7	181 $\pm$ 9	158 $\pm$ 7	25.7 $\pm$ 1.6
Co-crystal 1	Cells	2708 $\pm$ 84 (*)	301 $\pm$ 14 (*)	185 $\pm$ 11	21 $\pm$ 1 (**)	37.7 $\pm$ 1.5 (***)
Mixture 2	Cells	1047 $\pm$ 50	147 $\pm$ 10	183 $\pm$ 10	152 $\pm$ 7	24.4 $\pm$ 1.2
Co-crystal 2	Cells	1013 $\pm$ 38	145 $\pm$ 6	177 $\pm$ 9	159 $\pm$ 8	20.1 $\pm$ 0.9 (***)
Mixture 3	Cells	3.2 $\pm$ 0.1 (*)	--	180 $\pm$ 10	36 $\pm$ 2 (**)	24.8 $\pm$ 0.9
Cocrystal 3	Cells	442 $\pm$ 18 (*)	374 $\pm$ 16 (*)	183 $\pm$ 10	164 $\pm$ 8	33.6 $\pm$ 0.6 (***)
$\gamma$ -Indomethacin	Filter	1015 $\pm$ 45	429 $\pm$ 18 (*)	--	--	--

(\*)  $P < 0.001$  versus  $\gamma$ -indomethacin permeating across NCM460 cell monolayers

(\*\*)  $P < 0.001$  versus TEER at “time 0” (0 min)

(\*\*\*)  $P < 0.001$  versus absolute bioavailability of  $\gamma$ - indomethacin

## Caption of Figures

**Figure 1.** Schematic representation of indomethacin and the co-formers 2-hydroxy-4-methyl-pyridine in its keto form, 2-methoxy-5-nitroaniline and saccharine in co-crystals **1**, **2** and **3**, respectively.

**Figure 2.** (a) ORTEPIII view and atom numbering scheme for co-crystals **1**; (b) ORTEPIII view and atom numbering scheme for co-crystals **2**; (c) indomethacin-saccharine complex **3** (from Ref. 19).

Thermal ellipsoids are drawn at the 40% probability level. Hydrogen bonds are drawn as dashed lines.

**Figure 3.** DSC thermograms for indomethacin and its co-crystals.

**Figure 4.** Solubility and dissolution profiles in phosphate buffer 200 mM [A] and PBS 10 mM [B] at 37°C for  $\gamma$ -indomethacin as free drug, or co-crystallized, or mixed in the parent mixtures. Data are reported as the mean  $\pm$  S.D. of three independent experiments.

**Figure 5.** Permeation kinetics of indomethacin after introduction in the “Millicell” apical compartments of powders constituted by free  $\gamma$ -indomethacin, its co-crystals or the parent mixtures of  $\gamma$ -indomethacin with co-crystallizing agents. The permeations were analyzed across monolayers obtained by NCM460 cells. The permeation of free  $\gamma$ -indomethacin was analyzed across the Millicell filters alone (filter) or coated by monolayers. The cumulative amounts in the basolateral receiving compartments were linear within 60 min ( $r \geq 0.97$ ,  $P \leq 0.001$ ). The resulting slopes of the linear fits were used for the calculation of permeability coefficients ( $P_{app}$ ). All data are reported as mean  $\pm$  SD of three independent experiments.

**Figure 6.** [A] Elimination profile of indomethacin after 0.90 mg infusion to rats. The elimination followed an apparent first order kinetic, confirmed by the semilogarithmic plot reported in the inset ( $n = 8$ ,  $r = 0.983$ ,  $P < 0.0001$ ). The half-life of indomethacin was calculated to be  $8.94 \pm 0.38$  hours.

[B] Blood indomethacin concentrations ( $\mu\text{g/ml}$ ) after intravenous infusion (IV) or oral administration of 0.90 mg dose to rats within 24 hours. The oral formulations were constituted by the sieved powders of free  $\gamma$ -indomethacin, its co-crystals and the parent mixtures.

[C] Detailed blood indomethacin concentrations ( $\mu\text{g/ml}$ ) after oral administration of 0.90 mg dose to rats within 8 hours. All data reported in Figure are expressed as the mean  $\pm$  SD of four independent experiments.

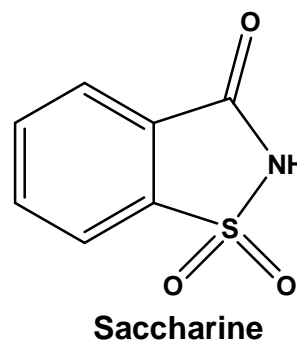
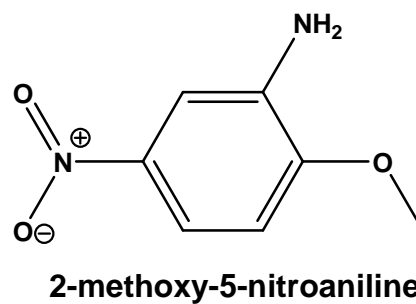
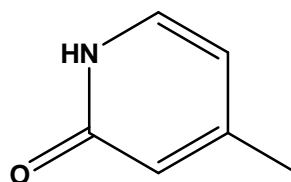
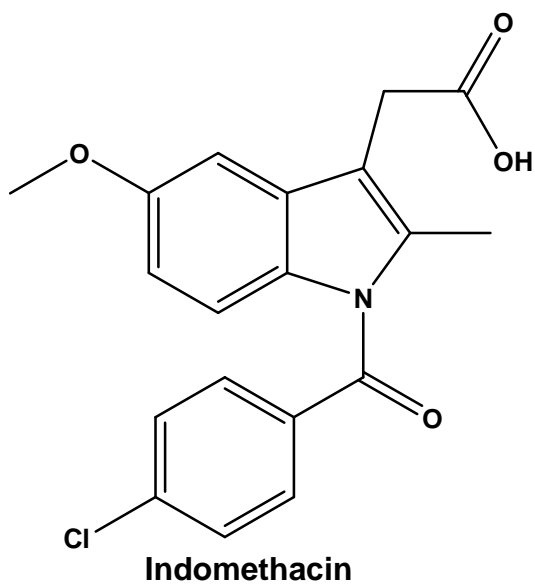


Figure 1

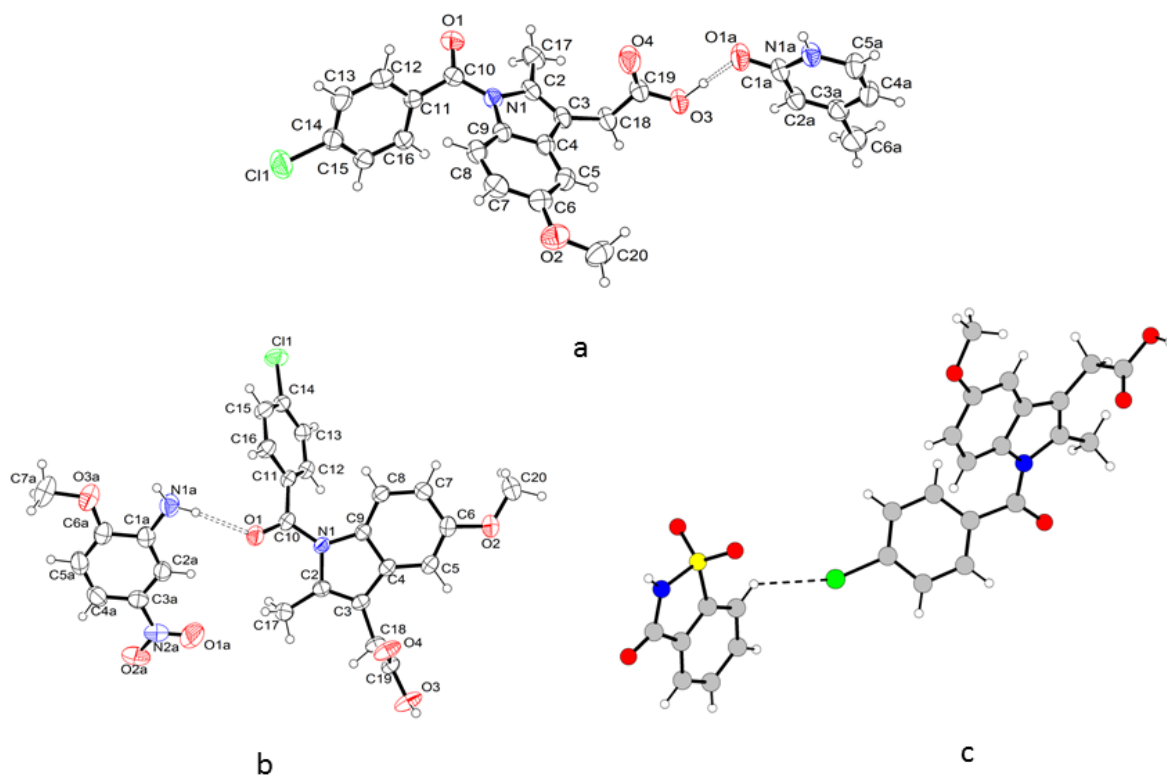
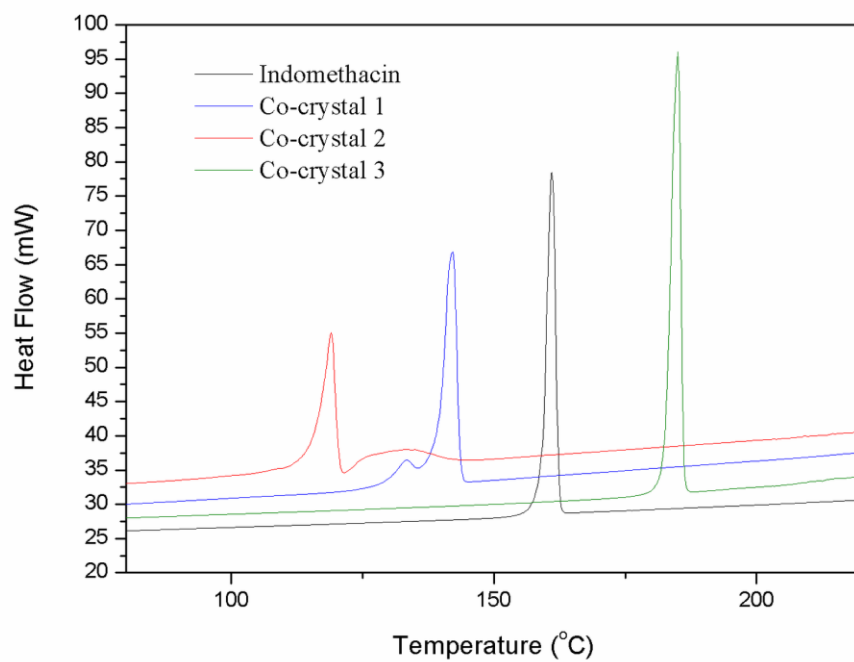
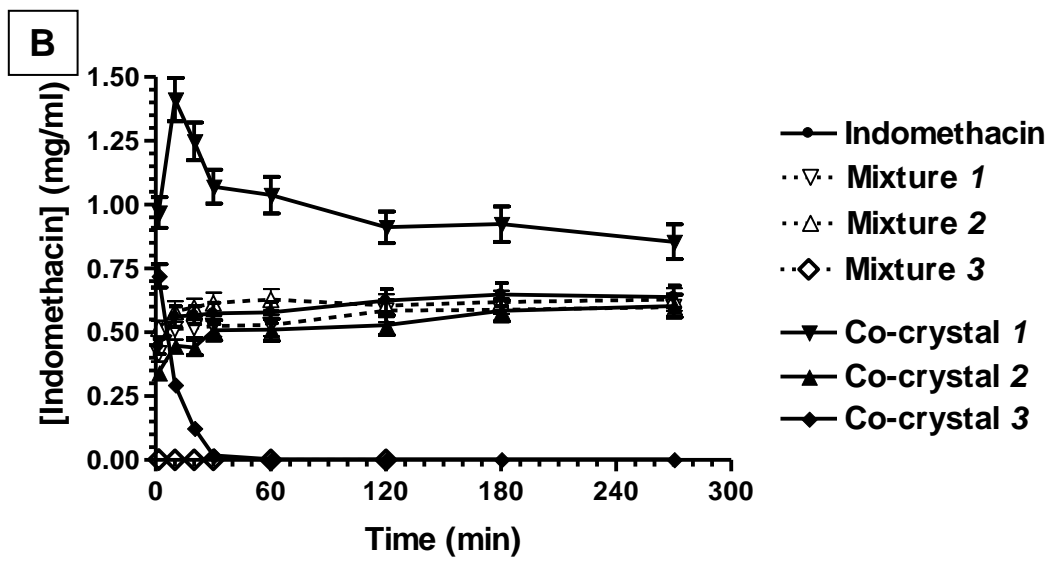
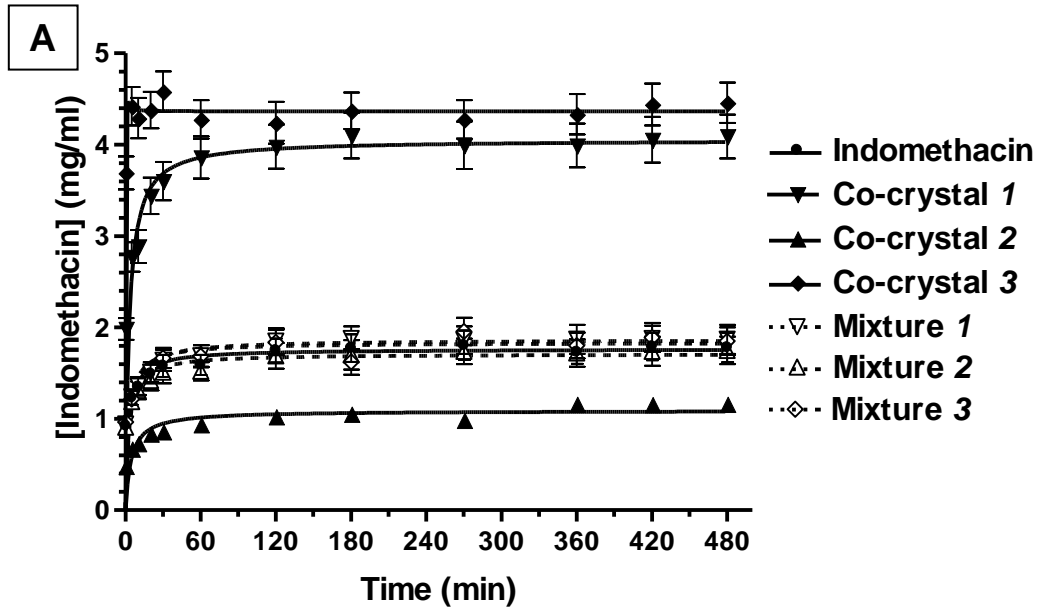


Figure 2



**Figure 3**



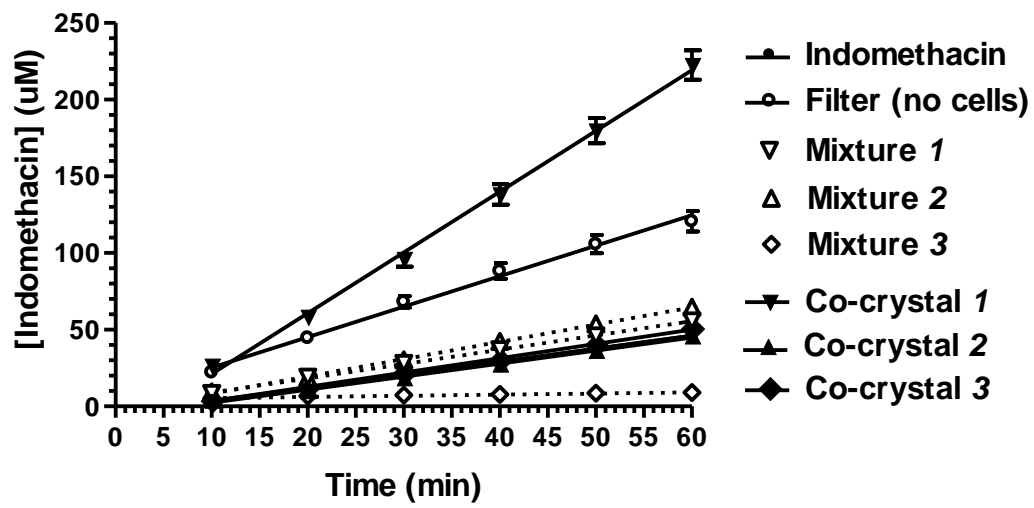


Figure 5

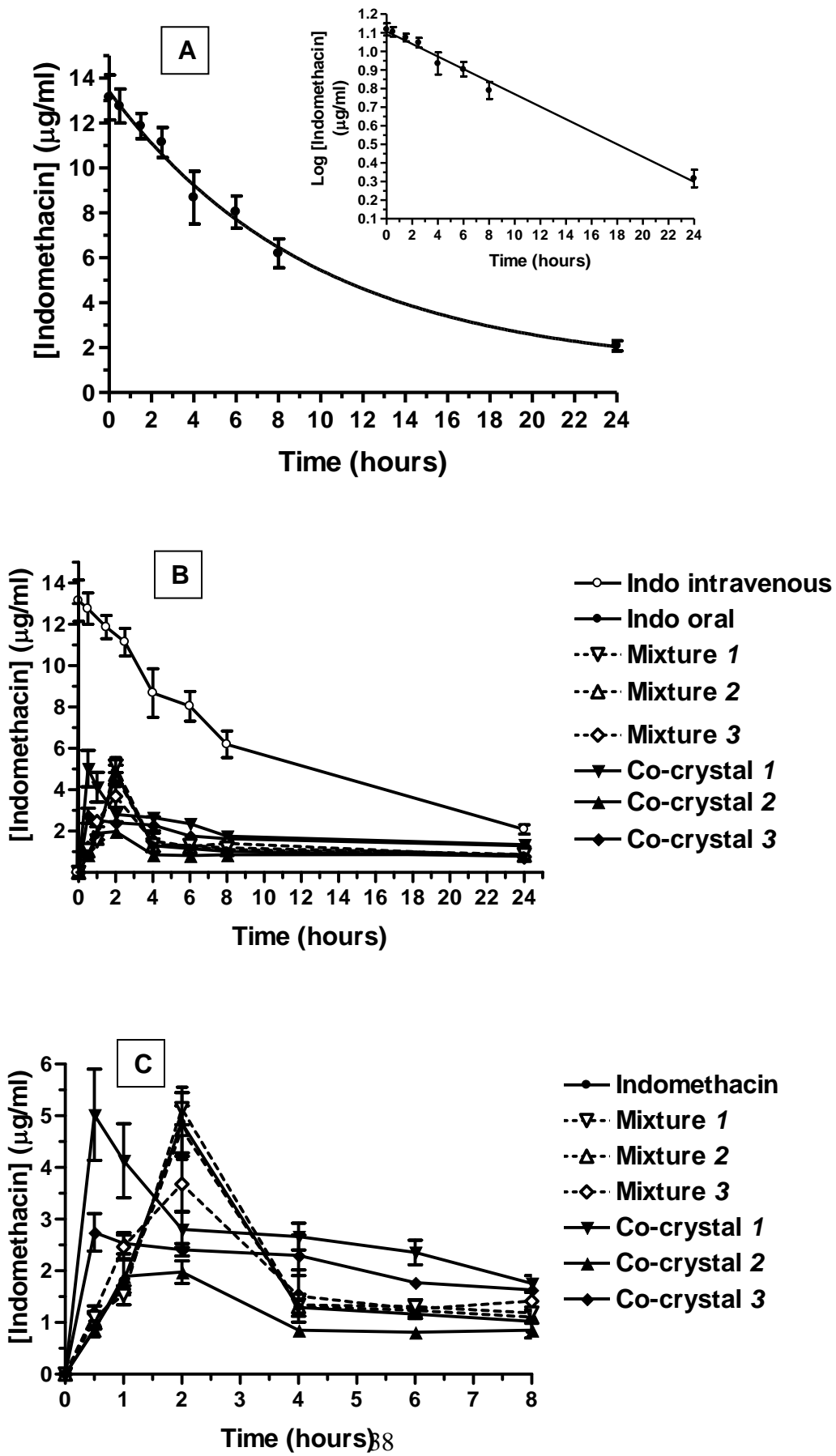


Figure 6